# Extracting Information on Linear and Nonlinear Absorption from 2-Beam Action Spectroscopy Data

Samuel R. Cohen[†] and John T. Fourkas[*, †,‡,§]

[†]Department of Chemistry & Biochemistry, [‡]Institute for Physical Science and Technology, [§]Maryland NanoCenter, [¶] Center for Nanophysics and Advanced Materials, University of Maryland, College Park, 20742, United States

ABSTRACT: 2-beam action (2-BA) spectroscopies are a recently developed class of techniques for determining the order(s) of absorption (1-photon, 2-photon, etc.) that contribute to an observable signal. When only a single order of absorption is present, 2-BA spectroscopies allow for the determination of that order by obtaining data at a single value of the observable. It has been shown previously that when two orders of absorption are present, they can be determined unambiguously by making measurements at several values of the observable. However, this latter approach cannot be used for single-valued observables, such as a polymerization threshold. Here we develop a theoretical comparison between conventional methods that determine the order(s) of absorption using logarithmic plots and 2-BA-based techniques. We also explore how 2-BA plots arising from two orders of absorption deviate from a plot with a single, non-integer exponent. We demonstrate that these deviations can usually be used to identify the two orders of absorption and their relative contributions to the signal based on measurements made at a single value of the observable.

## Introduction

Multiphoton absorption (MPA) is one of the most commonly used of nonlinear optical phenomena, particularly in ultrafast optics.[1-4] MPA is a powerful spectroscopic tool,[5-8] and is also a key enabling technology for applications such as fluorescence microscopy,[9-15] microfabrication,[16-22] and optical data storage.[23-26] As a result, it is desirable to be able to characterize nonlinear absorption (NLA) processes accurately. For instance, it is often advantageous to maximize the MPA cross section of molecules or materials to make the nonlinear absorption process as efficient as possible. Accurate determination of an MPA cross section requires knowledge of the order of nonlinear absorption, as well as of the nature of any competing processes, such as excited-state absorption[27-29] (ESA). Typical methods for characterizing MPA cannot reveal the contributions of multiple absorption pathways unambiguously.

NLA processes can be characterized either directly or indirectly. In the former case the transmission loss of a laser beam is measured.[30-32] Most direct techniques detect weak MPA over a large background signal, and so it is difficult to extract detailed information regarding complex photophysical or photochemical processes. Indirect methods rely on the detection of some proxy observable, such as emission or photocurrent, that is generated by MPA.[33-40] The most common method of measuring the order of NLA from either direct or indirect methods is to create a logarithmic plot of the observable as a function of irradiance. The order of NLA is determined from the slope of such a plot. However, the accurate determination of the order of absorption generally requires data that span two or more orders of magnitude in the irradiance.[41] Furthermore, it is common for non-integer slopes to be observed, in which case multiple orders of absorption and/or other processes such as ESA may be present. Unless considerable dynamic

range is available, logarithmic plots cannot be used to ascertain unambiguously which processes contribute to the observed signal or what the relative magnitudes of these contributions are.

Another approach for characterizing NLA is the Z-scan technique.[42-50] The Z-scan is a direct method in which loss is measured as a function of the distance of the sample from the laser focus. The order of MPA in a Z scan is determined by fitting the shape of the loss curve. Under favorable conditions, it is possible to ascertain the order of a single absorption process from a Z-scan measurement,[51-52] but the accurate determination of the influence of multiple processes is again challenging.

A further complication arises when MPA drives an irreversible process, particularly one, such as photopolymerization, that has an exposure threshold. Under such circumstances it is usually not possible to make logarithmic plots, and Z-scan studies are not feasible. The usual approach to this problem is to make measurements in a medium in which the reactivity of the excited species is unimportant, such as an inert solvent. However, there is no guarantee that the absorption process that is observed under such circumstances is the same as the one that leads to the irreversible phenomenon in the medium of interest. Alternative approaches that make measurements as a function of laser repetition rate[39] and/or exposure time[40] can also be used to glean insights into the order of NLA. Such methods still cannot provide an unambiguous description of the NLA process when multiple channels are involved.

We have recently developed a class of techniques that addresses many of the shortcomings of conventional methods for determining the effective order of NLA.[53-56] These methods, called 2-beam action (2-BA) spectroscopies, rely on using two temporally interleaved pulse trains to generate an observable by nonlinear and/or linear absorption. By finding different sets of average powers for the two pulse trains that lead to the same value of an observable, it is possible to

determine the effective order of NLA at that specific value of the observable. We have used this technique to probe NLA-induced observables including polymerization,[53,56] emission,[55] and photocurrent.[54]

As we have shown previously,[54] one of the advantages of 2-BA spectroscopies is that when multiple phenomena contribute to the measured exponent it is possible to determine the order and/or nature of these phenomena. The strategy that we demonstrated for elucidating the different contributions is to make 2-BA measurements at a range of values of the observable and then to test the results against a model. The above approach is only applicable when 2-BA measurements can be made at several values of an observable. There are many situations in which 2-BA measurements can only be made over a limited range of observable values. The extreme example of this situation is photopolymerization,[53] for which there is only one value of the observable (the threshold exposure dose).

Here we explore in more detail the relationship between the analysis of NLA via logarithmic plots and via 2-BA spectroscopy when there are two orders of absorption involved. We demonstrate that under these circumstances the standard equation used to fit 2-BA plots is only approximate. We examine six different combinations of orders of absorption, and show how the 2-BA plot deviates from an "ideal" 2-BA plot with a single, non-integer exponent as the relative contributions of the two orders are varied. Based on these results, we demonstrate how the orders and magnitudes of the two absorption contributions can usually be distinguished even if it is only possible to obtain data at one value of the observable.

## Theory

The concept of 2-BA spectroscopy is illustrated in Figure 1A. Two temporally interleaved pulse trains are incident upon the sample of interest at irradiances far below the saturation regime, generating an observable signal. If the delay time between two temporally adjacent pulses is long enough for the electronic excitation to relax completely, then the action of each pulse can be considered in isolation. The average power of one of the pulse trains (which we will call beam 1) required to attain a particular value of the observable is first determined. Beam 2 is then adjusted to have a non-zero average power, and the average power of beam 1 that returns the observable to its selected value is determined. This process is repeated until only beam 2 has non-zero average power.

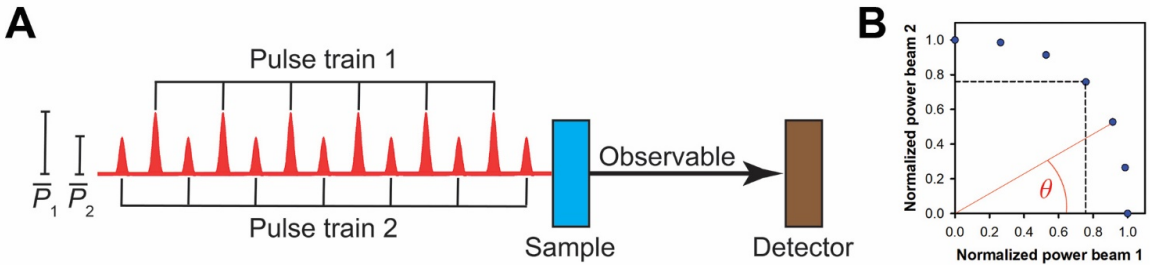


**Figure 1** (A) Schematic depiction of 2-beam action spectroscopy. Two temporally interleaved pulse trains with average powers $\bar{P}_1$ and $\bar{P}_2$ are incident on a sample, generating an observable via linear and/or nonlinear absorption. (B) Sets of values of $\bar{P}_1$ and $\bar{P}_2$ are determined that lead to the same value of the observable, and $\bar{P}_2$ is plotted as a function of $\bar{P}_1$ to determine the order(s) of absorption. The dashed lines denote $\bar{P}_{diag}$. $\theta$ is the angle a line from the origin to a data point makes with the *x* axis.

In principle, the average power at which each individual beam gives the desired value of the observable should be identical. In practice, these average powers may vary slightly. As a result, normalized powers are typically used in 2-BA spectroscopies, i.e. the average power of a given beam divided by the average power at which that beam alone yields the desired value of the observable. In this situation, for an *m*-photon absorption process the 2-BA data will adhere to the relation[53]

$$\bar{P}_1^m + \bar{P}_2^m = 1\,, \tag{1}$$

where the overbar indicates a normalized average power. Thus, *m* can be determined by plotting $\bar{P}_2$ as a function of $\bar{P}_1$ (Figure 1B). So long as only one order of absorption contributes to the observed signal, *m* will correspond to the order of that process, as will the slope of a logarithmic plot, *n*.

Now imagine that two different orders of absorption, *j* and *k*, where $j < k$, contribute to the observed signal. We will refer to this set of exponents henceforth as (*j*,*k*). In this situation the signal *S* will be given by

$$S(I) \propto AI^j + BI^k \,, \tag{2}$$

where *I* is the irradiance and *A* and *B* are constants that depend on factors such as the absorption cross sections of the different orders, the temporal shape of the laser pulses, and the quantum yield for the observable.[33] Note that *j*- and *k*-photon transitions using the same source wavelengths typically excite different states. In a traditional measurement, the slope of a logarithmic plot of the signal as a function of irradiance at a given irradiance *I* will then be given by

$$n = \frac{d\ln(S)}{d\ln(I)} = j + \Delta j \frac{BI^k}{AI^j + BI^k} \,, \tag{3}$$

where $\Delta j = k - j$.

Note that a given value of *n* could arise from any (*j*,*k*). The only way to identify these orders via a logarithmic plot is to collect data over a sufficient range of irradiance. However, the range of irradiance $\Delta I$ required to have the signal arise 90% from order *j* to 90% from order *k* is[54]

$$\Delta I = 81^{1/\Delta j} \,. \tag{4}$$

Thus, unless $\Delta j$ is large, it is essential to cover an order of magnitude or more in irradiance to be able to determine the orders of the absorption processes from a logarithmic plot.

In the case of 2-BA spectroscopy, the combination of two different orders of absorption leads to a plot that follows

$$a\left(\bar{P}_1^j + \bar{P}_2^j\right) + b\left(\bar{P}_1^k + \bar{P}_2^k\right) = 1\,, \tag{5}$$

where $a + b = 1$. This expression can be rearranged to give[54]

$$1 - \bar{P}_1^k - \bar{P}_2^k = a\left(\bar{P}_1^j + \bar{P}_2^j - \bar{P}_1^k - \bar{P}_2^k\right)\,. \tag{6}$$

This linearized equation can be used to determine $a$, and therefore $b$, at a single value of the observable. However, values of $a$ and $b$ can be found in principle for any ($j$,$k$).

We can interpret $a$ as being the fraction of the absorption arising from order $j$, which implies that

$$a = \frac{AI^j}{AI^j + BI^k}\,. \tag{7}$$

By the same token,

$$b = \frac{BI^k}{AI^j + BI^k}\,. \tag{8}$$

The ratio of the observable arising from order $k$ to that arising from order $j$ is therefore

$$\frac{b}{a} = \frac{BI^k}{AI^j} = \frac{B}{A} I^{\Delta j}\,. \tag{9}$$

Thus, if $j$ and $k$ have been chosen correctly a plot of $b/a$ as a function of $I^{\Delta j}$ will be linear with a slope of $B/A$ and will pass through the origin.[54] However, this approach requires that $a$ be able to be determined over a sufficient range of irradiance values.

**Results and Discussion**

We first consider the diagonal of a 2-BA plot, for which $\bar{P}_1 = \bar{P}_2 = \bar{P}_{diag}$ (Figure 1B). The simplest manner of determining the 2-BA exponent $m$, which we will call the 3-point method, is

to measure the values of $\bar{P}_1$ and $\bar{P}_2$ when only one beam is used and then to measure $\bar{P}_{diag}$. It follows from Eq 1 that

$$\bar{P}_{diag}^{m} = \frac{1}{2}. \tag{10}$$

Thus, we have that

$$m = \frac{\ln(1/2)}{\ln(\bar{P}_{diag})}. \tag{11}$$

In general, it is preferable to use more than three data points to determine *m*, although if the exponent is known to be an integer then the 3-point method should generally be sufficient. This strategy can be thought of as a variation of one developed by Wegener and coworkers to measure the effective order of nonlinear absorption in multiphoton absorption polymerization.[39]

When two orders of absorption contribute to the signal, Eq 5 leads to the relation

$$\bar{P}_{diag}^{k} + a\left(\bar{P}_{diag}^{j} - \bar{P}_{diag}^{k}\right) = \frac{1}{2}. \tag{12}$$

Combining Eq 10 and Eq 12 we find that

$$a = \frac{\bar{P}_{diag}^{m} - \bar{P}_{diag}^{k}}{\bar{P}_{diag}^{j} - \bar{P}_{diag}^{k}}. \tag{13}$$

Similarly,

$$b = \frac{\bar{P}_{diag}^{j} - \bar{P}_{diag}^{m}}{\bar{P}_{diag}^{j} - \bar{P}_{diag}^{k}}. \tag{14}$$

Thus, by determining *m* along the diagonal it is possible to find the values of *a* and *b* for a specific (*j*,*k*). By the same token, if *a*, *j*, and *k* are known then *m* can be found using the relation

$$m = \frac{\ln\left[\bar{P}_{diag}^{k} + a\left(\bar{P}_{diag}^{j} - \bar{P}_{diag}^{k}\right)\right]}{\ln(\bar{P}_{diag})}. \tag{15}$$

Furthermore, Eqs 3, 8, 10, and 14 can be combined to give an expression that allows the slope *n* of a logarithmic plot to be calculated from the 2-BA exponent *m* measured along the diagonal:

$$n = j + \Delta j \frac{1-2^{-(m-j)/m}}{1-2^{-\Delta j/m}}. \quad (16)$$

In Figure 2 we show the dependence of $n$ on $m$ for the six different ($j$,$k$) examined here. The general behavior that is observed in all cases is that $n < m$ for values below $j$ and above $k$, whereas $n > m$ for values between $j$ and $k$. When the exponent is either $j$ or $k$ then $n = m$. For values above $k$ the dependence of $n$ on $m$ is roughly linear. Unfortunately, Eq 16 cannot be inverted to find an expression for $m$ as a function of $n$. However, as shown below, specific expressions exist for $m$ as a function of $n$ for any given ($j$,$k$).

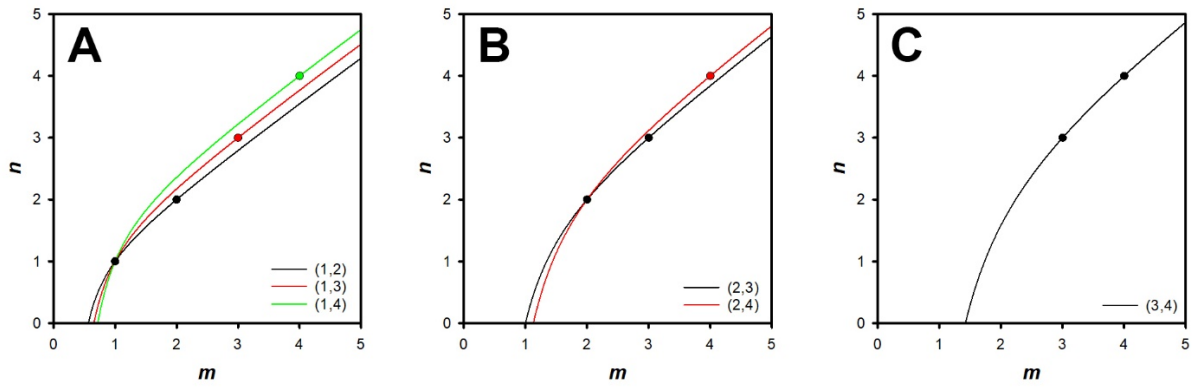


**Figure 2** Plots of the logarithmic plot exponent $n$ as a function of the 2-BA exponent $m$ for six different ($j$,$k$): (A) sets for $j$ = 1; (B) sets for $j$ = 2; and (C) the set for $j$ = 3. The symbols indicate the points at which $n = m$, which occurs when only a single absorption process is present.

Although the above strategy allows for the determination of $a$ from the value of $m$ measured along the diagonal, this method offers no direct means of determining what the correct ($j$,$k$) might be. Furthermore, if $a$ and $b$ are not zero, then in general the only places that data points for a specific value of $m$ will be equal to data points for a combination of two explicit orders of absorption will be along the axes and on the diagonal. However, the deviation of a plot for a single, non-integer exponent $m$ from a plot for an explicit ($j$,$k$) can provide a substantial amount of information about the true values of $j$ and $k$.

The simplest manner of measuring the deviation between two different 2-BA plots is to determine the radial distance between points that are at the same angle $\theta$ from the $x$ axis (see Figure 1b). In the case of a plot for a single exponent $m$, the slope $s$ of a line from the origin to a data point at angle $\theta$ is given by

$$s = \tan\theta = \frac{\bar{P}_2}{\bar{P}_1} . \tag{17}$$

Accordingly,

$$\bar{P}_2(\theta) = s\bar{P}_1(\theta) . \tag{18}$$

Plugging this result into Eq 1 leads to

$$\bar{P}_1(\theta) = \left(\frac{1}{1+s^m}\right)^{1/m} . \tag{19}$$

To find the coordinates of a data point at angle $\theta$ when there are contributions from two exponents, we begin by rewriting Eq 5 as

$$\left(\bar{P}_1^k + \bar{P}_2^k\right) + \frac{a}{1-a}\left(\bar{P}_1^j + \bar{P}_2^j\right) - \frac{1}{1-a} = 0 . \tag{20}$$

Combining this result with Eq 18 we find that

$$\bar{P}_1^k(\theta) + \frac{a(1+s^j)}{(1-a)(1+s^k)}\bar{P}_1^j(\theta) - \frac{1}{(1-a)(1+s^k)} = 0 . \tag{21}$$

The $x$ coordinate can be determined by finding the appropriate root of this polynomial, with the $y$ coordinate then following from Eq 18.

As an example, we consider the case in which $j = 1$ and $k = 2$. The polynomial for which we must find the root is

$$\bar{P}_1^2(\theta) + \frac{a(1+s)}{(1-a)(1+s^2)}\bar{P}_1(\theta) - \frac{1}{(1-a)(1+s^2)} = 0 . \tag{22}$$

The relevant root of this equation is

$$\bar{P}_1(\theta) = \frac{-a(1+s)+\sqrt{a^2(1+s)^2+4(1-a)(1+s^2)}}{2(1-a)(1+s^2)} . \tag{23}$$

Along the diagonal this equation becomes

$$\bar{P}_{diag}(\theta) = \frac{-a+\sqrt{a^2-2a+2}}{2(1-a)}. \tag{24}$$

Eqs 3 and 8 imply that

$$a = \frac{k-n}{\Delta j}. \tag{25}$$

By plugging this result into Eq 24 and then using Eq 11 we find that

$$m = \ln(1/2)/\ln\left(\frac{n-2+\sqrt{n^2-2n+2}}{2(n-1)}\right). \tag{26}$$

Thus, we are able to use this approach to determine *m* from *n* for this particular (*j*,*k*). Results of a corresponding analysis for the other five possible (*j*,*k*) with individual exponents ranging from 1 to 4 are given in the Supporting Information.

In Figure 3a we plot the difference between the (1,2) curve (from Eq 5) and the single effective exponent curve (from Eq 1) as a function of $\theta$ for values of *a* ranging from 0.1 to 0.9. The difference is symmetric about the diagonal, because the two beams are interchangeable. In all cases the deviation is negative, i.e. the plot with a single effective exponential extends a greater distance from the origin than the actual plot, except on the axes and on the diagonal. When *a* is close to 0 or 1, there is only a small contribution from one exponent, and the deviations are

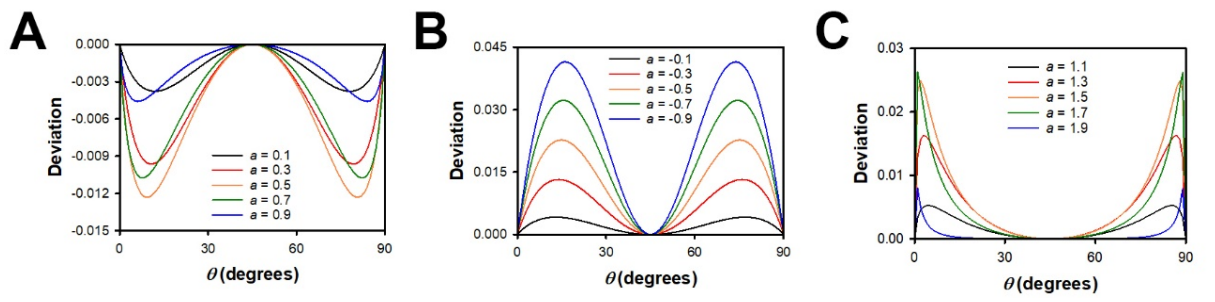


**Figure 3** The difference between Eq 5 and Eq 1 with *m* determined along the diagonal for a combination of linear and quadratic components as a function of the amplitude of the linear component, *a*. The panels show results for *a* values ranging from (A) 0.1 to 0.9; (B) -0.1 to -0.9; and (C) 1.1 to 1.9.

relatively small. The largest deviations are observed when $a$ = 0.5. In all cases the largest deviation is observed at an angle that lies in the range from roughly 5° to 15°. The larger the value of $a$, the smaller the angle at which the largest deviation is observed.

Although in most circumstances the contributions of two different orders of absorption are expected to be additive, it is also possible for them to be of opposite sign. One example of this situation would be a system in which linear absorption generates fluorescence, but 2-photon absorption populates a dark state. We should therefore also consider values of $a$ that are less than zero or greater than 1. We investigate the former case in Figure 3b for values of $a$ ranging from -0.1 to -0.9. In this case the deviation is positive, and grows in magnitude as $|a|$ increases. The angle of maximum deviation also increases as $|a|$ increases.

In Figure 3c we plot the deviation for values of $a$ ranging from 1.1 to 1.9. We note that when $a > 1$, the quantity $1 - a$ is negative, and so the other root of Eq 22 (with a negative sign before the square root) is used. This range of $a$ was chosen because the slope of a logarithmic plot is 0 when $a = 2$ (see Eq 25). In this case the deviation is also positive. The maximum deviation grows with increasing $a$, but becomes smaller again as $a$ approaches 2. The angle at which the maximum deviation occurs also decreases with increasing $a$.

Plots corresponding to Figure 3 for the five other pairs of combinations of exponents from 1 to 4 are given in the Supporting Information (Figures S1 to S5). The same general trends are observed for these other sets of exponents. The deviations are negative for $0 < a < 1$, and

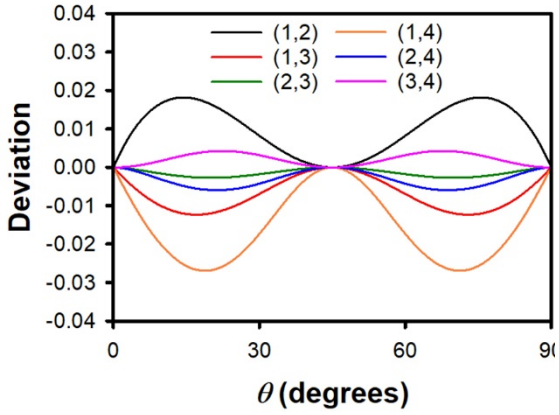


**Figure 4** The difference between Eq 5 and Eq 1 for $m$ = 2.5 for each of the different ($j$,$k$) examined.

generally positive for $a < 0$ and $a > 1$, although for large enough values of $a$ the deviations can become negative. The angle at which the maximum deviation occurs shifts in the same manner as $a$ is varied, but for fixed $a$ the angle at which the largest deviation occurs generally becomes larger as the exponents become larger. The magnitudes of the deviations are also dependent upon ($j$,$k$).

It is also useful to consider how the deviations for a fixed value of $m$ depend on ($j$,$k$). As a representative case, in Figure 4 we plot the deviations for $m = 2.5$ for the six different ($j$,$k$). Two general trends are apparent in this plot. First, the deviations are positive when $j$ and $k$ are both less than $m$ or both greater than $m$, and are negative when $m$ is between $j$ and $k$. Second, for deviations of the same sign, the magnitude of the deviation grows with the ratio $k/j$.

As discussed above, 2-BA spectroscopy data can generally be fit to Eq 6 for multiple ($j$,$k$). The correct values of $j$ and $k$ can be determined by determining $a$ and $b$ for different values of $m$ and finding which set of exponents is consistent with Eq 9. However, it is worthwhile to consider whether there are conditions under which ($j$,$k$) can be determined from data obtained for a single value of $m$, and what data are required to make such a determination. Making a measurement for a single value of $m$ requires fewer experiments than making measurements for multiple values. Furthermore, in the case of processes with thresholds, such as photopolymerization, it is not possible to make measurements at different values of $m$.

As a representative example, we consider the case in which $m = 2.1$. In Figure 5 we plot Eq 6 for data corresponding to (1,2). The data points are color-coded based on their angle relative to the $x$ axis in a 2-BA plot. Given any significant experimental uncertainty, the data could also be fit well to (2,3), (2,4), and (3,4). Equivalent plots for (1,3) and (2,3) are shown in Figures 6 and 7, respectively. In the former case, any combination other than (1,2) might reasonably fit the

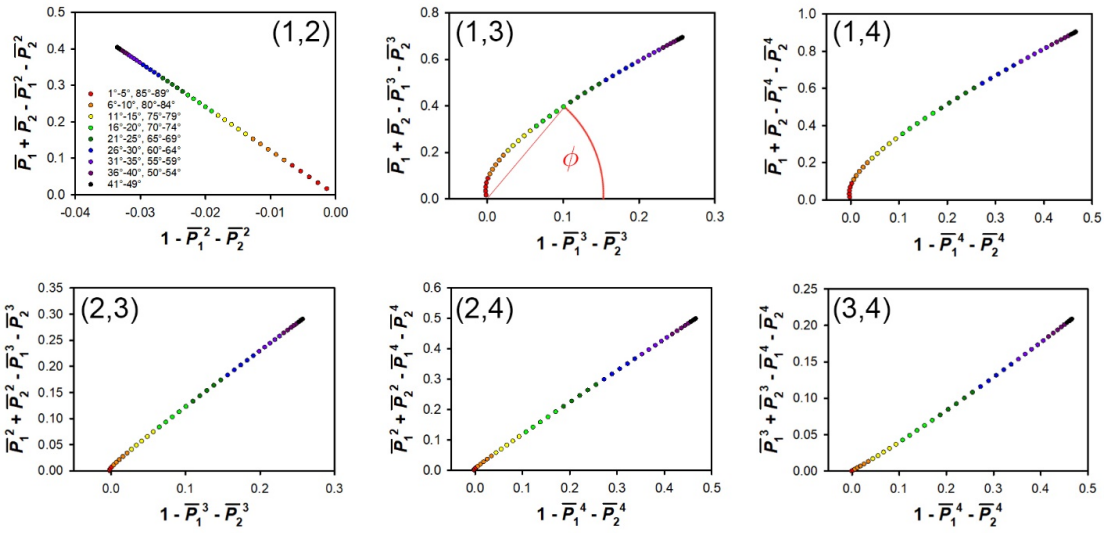


**Figure 5** Plots of Eq 6 using different ($j$,$k$) for data generated using (1,2) and $m$ = 2.1. The data points are color-coded based on their angle $\theta$ relative to the $x$ axis in a 2-BA plot (see legend). $\phi$ is the angle a line from the origin to a data point makes with the $x$ axis.

plots given a noise level that is typical experimentally. In the latter case, (1,3) could likely be ruled out as well. Plots for the other three combinations of $j$ and $k$ for $m$ = 2.1 are given in the Supporting Information (Figures S6 to S8).

Although the plots of Eq 6 for the specific ($j$,$k$) of interest do not always yield a clear sense of the appropriate sets of exponents, it should be noted that plots for other sets of exponents can be quite revealing. For instance, in the (2,3) case, the data points for plots for (1,2) are entirely in the second quadrant. However, in the (1,3) case, the data points for plots for (1,2) are in the first and second quadrants. Thus, even when a plot for a given $j$ and $k$ ends up not to be linear, it can still give insight into the actual values of ($j$,$k$). When $m$ is not an integer, it is therefore generally useful to make plots of Eq 6 for all six ($j$,$k$) explored here, even when not all of these ($j$,$k$) are physically plausible.

An additional approach that can be used to analyze 2-BA data that have a non-integer $m$ is to plot the angles that the data points in Eq 6 make with the $x$ axis ($\phi$) as a function of the angle $\theta$ derived from the 2-BA plot (see Figure 5). Such plots can complement plots of Eq 6, giving

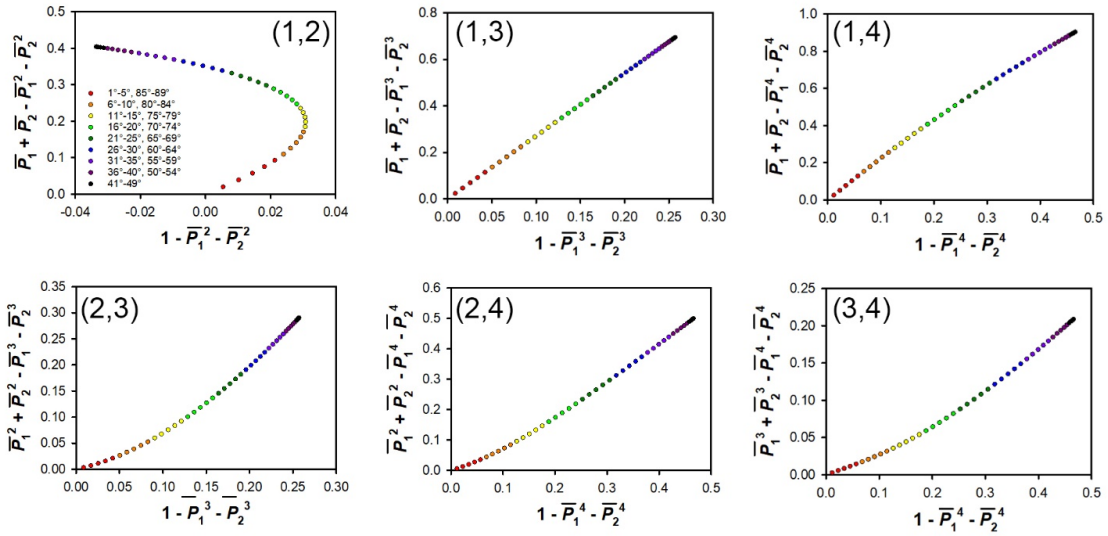


**Figure 6** Plots of Eq 6 using different (*j*,*k*) for data generated using (1,3) and $m = 2.1$. The data points are color-coded based on their angle $\theta$ relative to the $x$ axis in a 2-BA plot (see legend).

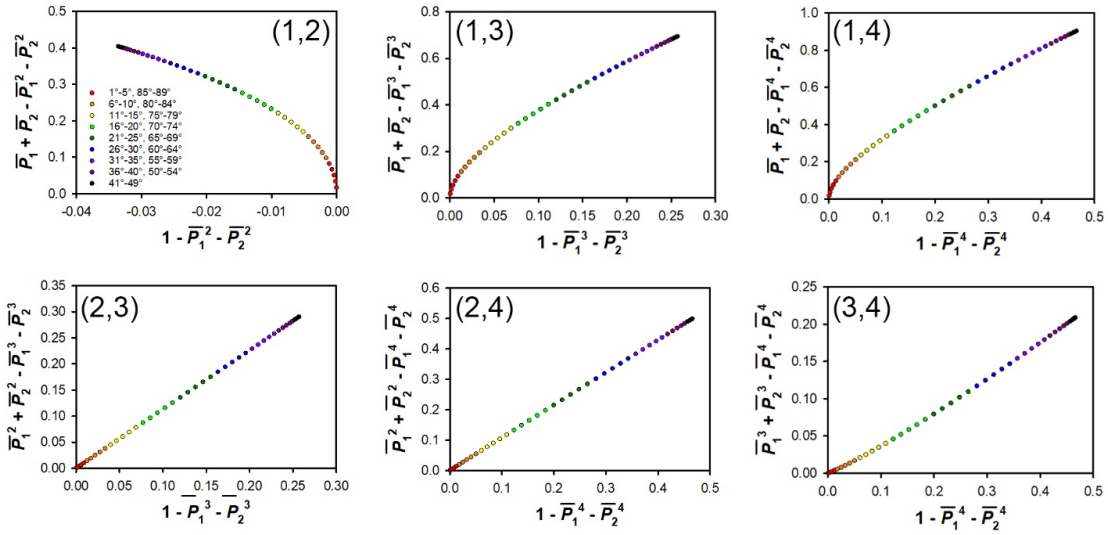


**Figure 7** Plots of Eq 6 using different (*j*,*k*) for data generated using (2,3) and $m = 2.1$. The data points are color-coded based on their angle $\theta$ relative to the $x$ axis in a 2-BA plot (see legend).

insight into which orders of absorption contribute to the signal in 2-BA spectroscopies. In many cases such plots in conjunction with plots of Eq 6 can lead to an unambiguous determination of two different orders of absorption that contribute to 2-BA spectroscopy data. As representative examples of this strategy, in Figure 8 we show the angular plots corresponding to the plots in Figures 5, 6, and 7. The corresponding plots for the other combinations of $j$ and $k$ for $m = 2.1$ are

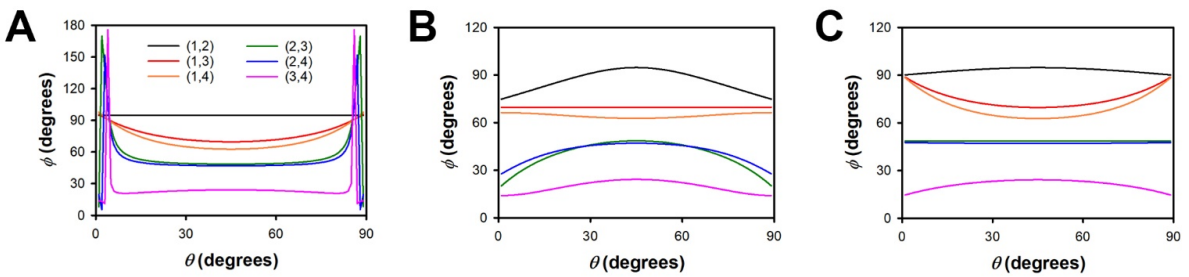


**Figure 8** The angle that plots of Eq 6 make with the $x$ axis ($\phi$) as a function of the 2-BA plot angle ($\theta$) for $m$ = 2.1 and different ($j$,$k$) using the data in (A) Figure 5; (B) Figure 6; and (C) Figure 7.

given in the Supporting Information (Figure S9). In conjunction with plots of Eq 6, these angular plots provide clear distinctions among different ($j$,$k$) in most cases, with the one exception in this example being that it remains difficult to tell the difference between (2,3) and (2,4).

Once a non-integer value of $m$ has been measured along the diagonal in a 2-BA spectroscopy experiment, it is useful to make plots of Eq 6 and the associated angular plots for the different ($j$,$k$) examined here. Such plots will reveal that angles at which 2-BA data will provide that greatest degree of discrimination among different possible ($j$,$k$). The most useful angles for measuring 2-BA data are typically ones at which there is a substantial deviation from linearity observable when incorrect ($j$,$k$) are tested.

## Conclusions

2-BA spectroscopies are a useful alternative to traditional logarithmic plots for determining the order(s) of absorption that contribute to an experimental observable. A measured exponent that is non-integral is generally indicative of a signal that is generated by two (or more) orders of absorption. In such situations, logarithmic plots and 2-BA plots yield a different effective exponent. We have developed a mathematical description of the relationships between these exponents for six different pairs of absorption orders: (1,2), (1,3), (1,4), (2,3), (2,4), and (3,4).

We have demonstrated previously how 2-BA measurements made at different values of the observable can be used to make an unambiguous determination of which two orders of absorption contribute to an observable.[54] However, in some circumstances the observable may be single-valued, as in the case of a photopolymerization threshold.[53] Here we have presented general principles for data analysis that, in most cases, can lead to the unambiguous determination of the orders of absorption at a single value of the observable. The crux of this strategy is the fact that 2-BA plots for pairs of contributions differ from "idealized" plots for a single, non-integer exponent. The form of this deviation is dependent upon the orders of absorption that contribute to the signal. Furthermore, analyzing 2-BA data assuming pairs of orders of absorption other than the pair that contributes to the signal can provide a characteristic signature of the actual orders of absorption.

Based on the results presented here, we suggest the following approach to analyzing 2-BA data. First, for a given value of the observable, the 3-point method should be used to determine the 2-BA exponent $m$ via Eq 11. At this point, the expected shapes of plots of Eq 6 and plots of $\phi$ as a function of $\theta$ can be determined. These plots will give guidance regarding the range of values of $\theta$ that will be most useful for distinguishing among different plausible ($j$,$k$). Additional 2-BA measurements can then be made in this range.

The ultimate success of this approach depends upon a number of factors. First, as discussed above, in some relatively rare cases this strategy on its own will not allow for distinction between two or three ($j$,$k$). However, practical considerations may still allow the appropriate set to be determined under such circumstances. Second, experimental uncertainty can be a limiting factor in such analysis. The higher the precision and accuracy of 2-BA data, the better the ability to distinguish among different ($j$,$k$). Finally, in some cases a 2-BA signal with a non-integer

exponent will not arise from two independent contributions. For instance, the observable may arise from two sequential contributions (e.g., absorption followed by ESA), or more than two contributions. Although the framework developed here does not describe such situations, in practice the inability to describe 2-BA data within this scheme can be taken to be indicative of the need for a more complex model. For non-cumulative observables (e.g., fluorescence and photocurrent, as opposed to photopolymerization) one way to test for phenomena such as thermal effects or interpulse ESA is to compare results when the beams are overlapped in space and when they are not overlapped in space. If the data are not the same in both cases then additional effects must be considered. We have shown previously how to model the signal in the presence of intrapulse ESA when there is also 2-photon and 3-photon absorption,[55] and similar approaches can be used for related cases.

**Associated content**

Supporting information: Equations for *m* as a function of *n* and for (1,3), (1,4), (2,3), (2,4), and (3,4), the deviations between a plot of a non-integer *m* and the corresponding plots for two different integer exponents as a function of *a* for (1,3), (1,4), (2,3), (2,4), and (3,4), plots of Eq 6 for the different (*j*,*k*) for data based on (1,4), (2,4), and (2,3), and angular plots for (1,4), (2,4), and (2,3). This material is available free of charge via the Internet at http://pubs.acs.org.

AUTHOR INFORMATION

**Corresponding author**

* E-mail: fourkas@umd.edu

* Phone: John T. Fourkas (301) 405-7996

## Notes

These authors declare no competing financial interest.

ACKNOWLEDGMENTS

This work was supported by the National Science Foundation, grant CHE-1800491.

## References

1. Bhawalkar, J. D.; He, G. S.; Prasad, P. N., Nonlinear Multiphoton Processes in Organic and Polymeric Materials. *Rep. Prog. Phys.* **1996**, *59*, 1041-1070.

2. He, G. S.; Tan, L. S.; Zheng, Q.; Prasad, P. N., Multiphoton Absorbing Materials: Molecular Designs, Characterizations, and Applications. *Chem. Rev.* **2008**, *108*, 1245-1330.

3. Liaros, N.; Fourkas, J. T., The Characterization of Absorptive Nonlinearities. *Laser Photon. Rev.* **2017**, *11*, 1700106.

4. Rumi, M.; Perry, J. W., Two-Photon Absorption: An Overview of Measurements and Principles. *Adv. Opt. Photon.* **2010**, *2*, 451-518.

5. Frohlich, D.; Sondergeld, M., Experimental Techniques in Two-Photon Spectroscopy. *J. Phys. E* **1977**, *10*, 761-766.

6. Friedrich, D. M.; McClain, W. M., Two-Photon Molecular Electronic Spectroscopy. *Annu. Rev. Phys. Chem.* **1980**, *31*, 559-577.

7. Birge, R. R., Two-Photon Spectroscopy of Protein-Bound Chromophores. *Acc. Chem. Res.* **1986**, *19*, 138-146.

8. Dai, H. L.; Kung, A. H.; Moore, C. B., Resonant Multi-Photon Dissociation and Mechanism of Excitation for Ethyl Chloride. *Phys. Rev. Lett.* **1979**, *43*, 761-764.

9. Carriles, R.; Schafer, D. N.; Sheetz, K. E.; Field, J. J.; Cisek, R.; Barzda, V.; Sylvester, A. W.; Squier, J. A., Imaging Techniques for Harmonic and Multiphoton Absorption Fluorescence Microscopy. *Rev. Sci. Instrum.* **2009**, *80*, 081101.

10. Denk, W.; Strickler, J.; Webb, W., Two-Photon Laser Scanning Fluorescence Microscopy. *Science* **1990**, *248*, 73-76.

11. Diaspro, A.; Robello, M., Two-Photon Excitation of Fluorescence for Three-Dimensional Optical Imaging of Biological Structures. *J. Photochem. Photobiol. B* **2000**, *55*, 1-8.

12. Kirejev, V.; Guldbrand, S.; Borglin, J.; Simonsson, C.; Ericson, M. B., Multiphoton Microscopy - A Powerful Tool in Skin Research and Topical Drug Delivery Science. *J. Drug Deliv. Sci. Technol.* **2012**, *22*, 250-259.

13. Schrader, M.; Bahlmann, K.; Hell, S. W., Three-Photon-Excitation Microscopy: Theory, Experiment and Applications. *Optik* **1997**, *104*, 116-124.

14. So, P. T. C.; Dong, C. Y.; Masters, B. R.; Berland, K. M., Two-Photon Excitation Fluorescence Microscopy. *Annu. Rev. Biomed. Eng.* **2000**, *2*, 399-429.

15. Wang, B. G.; Konig, K.; Halbhuber, K. J., Two-Photon Microscopy of Deep Intravital Tissues and its Merits in Clinical Research. *J. Microsc.* **2010**, *238*, 1-20.

16. LaFratta, C. N.; Fourkas, J. T.; Baldacchini, T.; Farrer, R. A., Multiphoton Fabrication. *Angew. Chem. Int. Ed.* **2007**, *46*, 6238-6258.

17. Stampfl, J.; Liska, R.; Ovsianikov, A., *Multiphoton Lithography: Techniques, Materials and Applications*. Wiley-VCH: Weinheim, 2017.

18. Baldacchini, T., *Three-Dimensional Microfabrication Using Two-Photon Polymerization*. Elsevier: Amsterdam, 2016.

19. Maruo, S.; Fourkas, J. T., Recent Progress in Multiphoton Microfabrication. *Laser Photon. Rev.* **2008**, *2*, 100-111.

20. Yang, D.; Jhaveri, S. J.; Ober, C. K., Three-Dimensional Microfabrication by Two-Photon Lithography. *MRS Bull.* **2005**, *30*, 976-982.

21. Farsari, M.; Vamvakaki, M.; Chichkov, B. N., Multiphoton Polymerization of Hybrid Materials. *J. Opt.* **2010**, *12*.

22. Sugioka, K.; Cheng, Y., Femtosecond Laser Three-Dimensional Micro- and Nanofabrication. *Appl. Phys. Rev.* **2014**, *1*, 041303.

23. Iliopoulos, K.; Krupka, O.; Gindre, D.; Salle, M., Reversible Two-Photon Optical Data Storage in Coumarin-Based Copolymers. *J. Amer. Chem. Soc.* **2010**, *132*, 14343-5.

24. Olson, C. E.; Previte, M. J.; Fourkas, J. T., Efficient and Robust Multiphoton Data Storage in Molecular Glasses and Highly Crosslinked Polymers. *Nat. Mater.* **2002**, *1*, 225-8.

25. Parthenopoulos, D. A.; Rentzepis, P. M., Three-Dimensional Optical Storage Memory. *Science* **1989**, *245*, 843-5.

26. Strickler, J. H.; Webb, W. W., 3-Dimensional Optical Data Storage in Refractive media by 2-Photon Point Excitation. *Opt. Lett.* **1991**, *16*, 1780-1782.

27. Giuliano, C.; Hess, L., Nonlinear Absorption of Light: Optical Saturation of Electronic Transitions in Organic Molecules with High Intensity Laser Radiation. *IEEE J. Quantum Electron.* **1967**, *3*, 358-367.

28. Sutherland, R. L.; Brant, M. C.; Heinrichs, J.; Rogers, J. E.; Slagle, J. E.; McLean, D. G.; Fleitz, P. A., Excited-State Characterization and Effective Three-Photon Absorption Model of Two-Photon-Induced Excited-State Absorption in Organic Push-Pull Charge-Transfer Chromophores. *J. Opt. Soc. Amer. B* **2005**, *22*, 1939-1948.

29. Zou, X.; Izumitani, T., Spectroscopic Properties and Mechanisms of Excited State Absorption and Energy Transfer Upconversion for $Er^{3+}$-Doped Glasses. *J. Non-Cryst. Solids* **1993**, *162*, 68-80.

30. Bechtel, J. H.; Smith, W. L., Two-Photon Absorption in Semiconductors with Picosecond Laser Pulses. *Phys. Rev. B* **1976**, *13*, 3515-3522.

31. Ehrlich, J. E.; Wu, X. L.; Lee, I. Y. S.; Hu, Z. Y.; Röckel, H.; Marder, S. R.; Perry, J. W., Two-Photon Absorption and Broadband Optical Limiting with bis-Donor Stilbenes. *Opt. Lett.* **1997**, *22*, 1843-1845.

32. Tian, P.; Warren, W. S., Ultrafast Measurement of Two-Photon Absorption by Loss Modulation. *Opt. Lett.* **2002**, *27*, 1634-1636.

33. Xu, C.; Webb, W. W., Measurement of Two-Photon Excitation Cross Sections of Molecular Fluorophores with Data from 690 to 1050 nm. *J. Opt. Soc. Amer. B* **1996**, *13*, 481-491.

34. Xu, C.; Williams, R. M.; Zipfel, W.; Webb, W. W., Multiphoton Excitation Cross-Sections of Molecular Fluorophores. *Bioimaging* **1996**, *4*, 198-207.

35. Twarowski, A. J.; Kliger, D. S., Multiphoton Absorption Spectra using Thermal Blooming. *Chem. Phys.* **1977**, *20*, 253-258.

36. White, W. T.; Henesian, M. A.; Weber, M. J., Photothermal-Lensing Measurements of Two-Photon Absorption and Two-Photon-Induced Color Centers in Borosilicate Glasses at 532 nm. *J. Opt. Soc. Amer. B* **1985**, *2*, 1402-1408.

37. Fang, H. L.; Gustafson, T. L.; Swofford, R. L., Two-Photon Absorption Photothermal Spectroscopy using a Synchronously Pumped Picosecond Dye Laser. Thermal Lensing Spectra of Naphthalene and Diphenylbutadiene. *J. Chem. Phys.* **1983**, *78*, 1663-1669.

38. Streltsov, A. M.; Moll, K. D.; Gaeta, A. L.; Kung, P.; Walker, D.; Razeghi, M., Pulse Autocorrelation Measurements Based on Two- and Three-Photon Conductivity in a GaN Photodiode. *Appl. Phys. Lett.* **1999**, *75*, 3778-3780.

39. Fischer, J.; Mueller, J. B.; Kaschke, J.; Wolf, T. J.; Unterreiner, A. N.; Wegener, M., Three-Dimensional Multi-Photon Direct Laser Writing with Variable Repetition Rate. *Opt. Express* **2013**, *21*, 26244-60.

40. Mueller, J. B.; Fischer, J.; Mayer, F.; Kadic, M.; Wegener, M., Polymerization Kinetics in Three-Dimensional Direct Laser Writing. *Adv. Mater.* **2014**, *26*, 6566-71.

41. Clauset, A.; Shalizi, C. R.; Newman, M. E. J., Power-Law Distributions in Empirical Data. *SIAM Rev.* **2009**, *51*, 661-703.

42. Sheik-Bahae, M.; Said, A. A.; Wei, T. H.; Hagan, D. J.; Van Stryland, E. W., Sensitive Measurement of Optical Nonlinearities using a Single Beam. *IEEE J. Quantum Electron.* **1990**, *26*, 760-769.

43. Ma, H.; Gomes, A. S. L.; de Araujo, C. B., Measurements of Nondegenerate Optical Nonlinearity using a Two-Color Single Beam Method. *Appl. Phys. Lett.* **1991**, *59*, 2666-2668.

44. Sheik-Bahae, M.; Wang, J.; DeSalvo, R.; Hagan, D. J.; Van Stryland, E. W., Measurement of Nondegenerate Nonlinearities using a Two-Color Z Scan. *Opt. Lett.* **1992**, *17*, 258-260.

45. Balu, M.; Hales, J.; Hagan, D. J.; Van Stryland, E. W., White-Light Continuum Z-Scan Technique for Nonlinear Materials Characterization. *Opt. Express* **2004**, *12*, 3820-3826.

46. Xia, T.; Hagan, D. J.; Sheik-Bahae, M.; Van Stryland, E. W., Eclipsing Z-Scan Measurement of $\lambda/10^4$ Wave-Front Distortion. *Opt. Lett.* **1994**, *19*, 317-319.

47. Petrov, D. V., Reflection Z-Scan Technique for the Study of Nonlinear Refraction and Absorption of a Single Interface and Thin Film. *J. Opt. Soc. Amer. B* **1996**, *13*, 1491-1498.

48. Petrov, D. V.; Gomes, A. S. L.; de Araújo, C. B., Reflection Z-Scan Technique for Measurements of Optical Properties of Surfaces. *Appl. Phys. Lett.* **1994**, *65*, 1067-1069.

49. Sengupta, P.; Balaji, J.; Banerjee, S.; Philip, R.; Kumar, G. R.; Maiti, S., Sensitive Measurement of Absolute Two-Photon Absorption Cross Sections. *J. Chem. Phys.* **2000**, *112*, 9201-9205.

50. Castro, H. P. S.; Pereira, M. K.; Ferreira, V. C.; Hickmann, J. M.; Correia, R. R. B., Optical Characterization of Carbon Quantum Dots in Colloidal Suspensions. *Opt. Mater. Express* **2017**, *7*, 401-408.

51. He, J.; Qu, Y.; Li, H.; Mi, J.; Ji, W., Three-Photon Absorption in ZnO and ZnS Crystals. *Opt. Express* **2005**, *13*, 9235-9247.

52. Corrêa, D. S.; De Boni, L.; Misoguti, L.; Cohanoschi, I.; Hernandez, F. E.; Mendonça, C. R., Z-Scan Theoretical Analysis for Three-, Four- and Five-Photon Absorption. *Opt. Commun.* **2007**, *277*, 440-445.

53. Tomova, Z.; Liaros, N.; Gutierrez Razo, S. A.; Wolf, S. M.; Fourkas, J. T., In Situ Measurement of the Effective Nonlinear Absorption Order in Multiphoton Photoresists. *Laser Photon. Rev.* **2016**, *10*, 849-854.

54. Liaros, N.; Cohen, S. R.; Fourkas, J. T., Determination of the Contributions of Two Simultaneous Absorption Orders using 2-Beam Action Spectroscopy. *Opt. Express* **2018**, *26*, 9492-9501.

55. Liaros, N.; Razo, S. A. G.; Fourkas, J. T., Probing Multiphoton Photophysics Using Two-Beam Action Spectroscopy. *J. Phys. Chem. A* **2018**, *122*, 6643-6653.

56. Zandrini, T.; Liaros, N.; Jiang, L. J.; Lu, Y. F.; Fourkas, J. T.; Osellame, R.; Baldacchini, T., Effect of the Resin Viscosity on the Writing Properties of Two-Photon Polymerization. *Opt. Mater. Express* **2019**, *9*, 2601-2616.

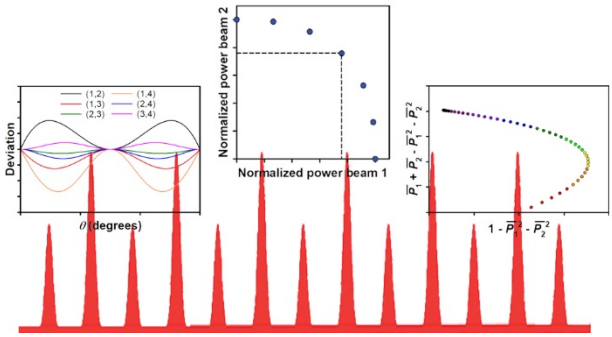
(1,2)
(1,3)
(2,3)
(1,4)
(2,4)
(3,4)
Deviation
(degrees)
Normalized power beam 2
Normalized power beam 1
1 - $\bar{P}_1^2$ - $\bar{P}_2^2$

# TOC graphic